Removal of Fine Particles on a Wall by High-Frequency Turbulence Added Air Flow

Kazuhiko Soemoto[1], Tatsuro Wakimoto[2] and Kenji Katoh[2]
[1]Shinko.Co.Ltd, Minamiokajima 5-8-84, Taisho-ku, Osaka-shi, Osaka 551-0021, Japan
[2]Graduate School of Engineering, Osaka City University,
Sugimoto 3-3-138, Sumiyoshi-ku, Osaka-shi Osaka 558-8585, Japan

Received date 2nd November 2012; Accepted date 27th February 2013

Abstract
A cleaning technique to remove particles of several micro-meter diameter from a surface under dry environmental conditions is greatly needed in the manufacturing processes of LCDs. However, it is usually difficult to remove the fine particles by simple airflow because the particles adhere to the surface by strong forces. For this reason, a cleaning device equipped with a special nozzle is used in the actual industrial process. The nozzle has triangular cavities to add strong high-frequency fluctuations to the airflow. To clarify the effect of this fluctuation on particle removal quantitatively, we measured the airflow velocity, pressure fluctuation on a surface, and removal ratio for four types of nozzles: two varieties cavity nozzles and two straight nozzles with different lengths. The correlation between the intensity of pressure or velocity fluctuation and removal ratio for the cavity nozzles suggests that the turbulent fluctuation added by the cavity contributes to particle removing.

1. INTRODUCTION
The liquid crystal display (LCD) technology is becoming increasingly widespread for home use in televisions and similar entertainment devices. The current trend in this industry is to produce larger mother glass sizes because production cost can be cut down by the increasing of the number of final products which are divided from a sheet of a mother glass; recently the production of 10th generation mother glass (Dimensions: 2850×3050mm) has begun. The most important issue in this industry concerns increasing yielding percentage of the large mother glass in order to remain competitive. Therefore, the industry is interested in improving the technology to remove fine particles from the glass surfaces during the manufacturing process.

One of the most important technologies in the semiconductor industry is the process of wet cleaning. However, this process has environmental issues due to the high volume of chemicals used. Therefore a dry cleaning process would be beneficial to this industry.

Dry cleaning using airflow technology would reduce these environmental problems. A device using this technology could potentially clean a large surface and minimize the use of complicated technology. However, there are currently two problems. One is that it becomes difficult to remove the fine particles by using a simple high-speed airflow when they are less than 10μm, because they are submerged in a viscous sublayer and are adhered to the wall by strong forces such as Van der Waals force. The other is that the supplied air flow rate increases in relation to the upsizing of the cleaning work surface.

Several experiments have been conducted to improve the removal of these micron-order fine particles. Gotoh *et al*. removed the fine particles using the impingement of an air jet ejected from a slit nozzle at 100-600kPa and measured the particle removal rate by counting particles before and after the process. Additionally they showed that the removal rate is affected by factors such as humidity, particle diameter, wall material, and impinging angle [1-4] . According to the reports, normal impingement of a jet is preferable for high removal rate and easy manufacturing. Otani *et al*. and Namiki *et al*. demonstrated that an intermittent air jet is effective for the removal of sub-micrometer particles [5-6]. Additionally, Schlosser *et al*. calculated the minimum diameter of the particle that can be removed by estimating the strengths of Van der Waals force and other removal forces such as aerodynamic force

[7]. Their calculations suggest that ultrasonic acoustic waves could potentially remove the fine particles.

In these experiments, a compressor was used to generate the air jet. However, the use of a compressor is unrealistic for actual industrial application because the compressor cannot discharge a large enough flow volume to clean a glass substrate for a 10th generation LCD within a short tact time.

One of the current technologies used in the industry to solve this problem is a cleaner with a specially designed air nozzle. The air nozzle has cavities inside designed to add fluctuations over 5 kHz to the air jet that is ejected from the blower. This occurs even at relatively low pressures such as 10kPa. Despite this, there are no prior works that have researched the main factors that determine the particle removal rate of the cleaner actually used in industry.

So, in this study, we measured the airflow velocity, velocity fluctuation, wall-pressure fluctuation and particle removal rate for three types of nozzles having 0.4 mm slit width. And we considered the factors that had the most significant effect on the removal rate.

In addition to the 0.4 mm slit nozzles, we manufactured a cavity nozzle having a 0.2 mm slit width to reduce the air flow rate and examined its removal ability under the same pressure conditions.

2. EXPERIMENTAL METHOD

2.1 Cleaning device

Figure 1(a) shows the cleaner head① and test plate⑤ used in this experiment. The cleaner head of 500mm length has a rectangular parallelepiped shape with a uniform section, and it is composed of an air storage chamber③ and two suction chambers⑦. Air is supplied and suctioned by a vortex blower (VB-060-E2: Hitachi Industrial Equipment Systems) through an inlet② and outlet⑧ mounted on the side face of the cleaner head. The air supplied to the air storage chamber is ejected from an exchangeable nozzle④ of 480mm length. The details of its nozzles construction are as shown in Fig. 1(b). The ejected air jet impinges on an acrylic test plate located below the nozzle exit. This jet removes particles⑥ that are subsequently sucked into the suction chambers connecting to the exhaust. The suction chambers have slits of 2mm width and 7mm depth on both sides 30mm away from the jet flow center.

In this experiment, the test plate had 400mm length, 200mm width, and 20mm thickness. A pressure tap⑩ of 0.5mm diameter was installed in the test plate for the pressure measurement (mentioned later) and was moved to the desired positions using a traverser⑫ that was equipped with dial gauges⑪ which determined the positions of the pressure tap with an accuracy of 0.01mm. The origin of the coordinates is a point on the wall under the center of the discharge slit, as shown in Fig.1 (a). Measurements along the x axis describe those that are along this wall.

The test plate and cleaner head were supported separately to avoid the transmission of mechanical vibration from the cleaner head. Dial gauges were then installed in the cleaner head to adjust the gap between the test plate and cleaner head (H). In this experiment a value of H=1.5mm was used. This measurement had an accuracy of 0.01mm. The both ends of the gap are opening to atmosphere.

During the experiment, we monitored the gauge pressure P in the air storage chamber with a manometer⑨ (PG-100-102RP: Copal Electronics) and controlled it with an inverter equipped with the blower. The pressure P was set to be 8kPa, 11kPa and 14kPa. The pressure of the suction chamber was maintained to be -1kPa. This negative pressure plays the only role for collecting floating particles from the wall surface and it rarely contributes particle removal directly because it is small compared with the exhalation pressure P. For this reason, the position of the suction slit rarely affects on the particle removal either. In these pressure conditions and apparatus dimensions, the flow rate of suction is greater than that of the exhalation. This quantity difference prevents the leak of the particles from the both ends of the gap and ensures the capture of the floating particles.

We tested four different types of nozzles as shown in Fig. 1(b) under the above pressure conditions. The SL (Straight Long) nozzle had a preliminary linear flow channel of 1.0mm width and 15mm depth before the discharge slit, and the SS (Straight Short) nozzle had a linear flow channel of 4.0mm width and 3.0mm depth. Due to its shape, the preliminary flow channel was minimized in the SS nozzle. The C (Cavity) and C' nozzle had two cavities with a triangular geometry (3.0mm width and 3.0mm depth) in two different places. Otherwise it was similar to the SL nozzle. The triangular cavities installed in both C and C' nozzles had a structure designed to add high frequency fluctuations to the flow. These fluctuations were generated by a feedback mechanism caused by vortexes interacting with the separated shear layer at the edge of the cavity. [8] As shown in Fig. 1(b), all three kinds of nozzles except C' have

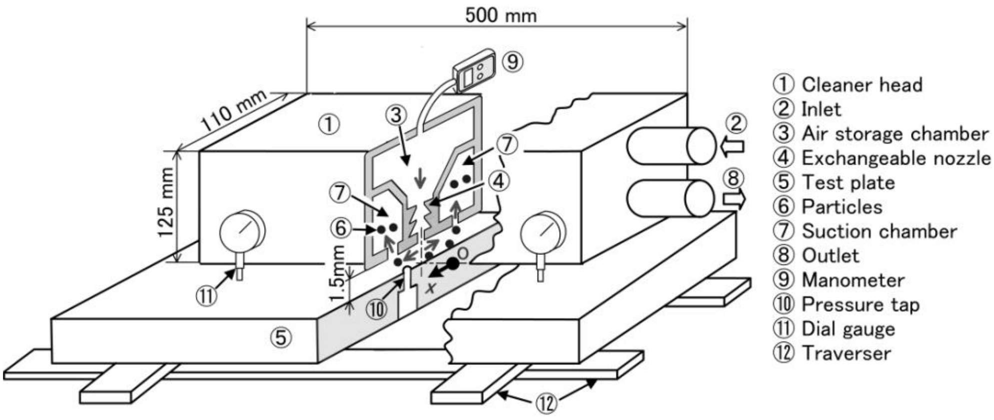

(a) Cleaning device

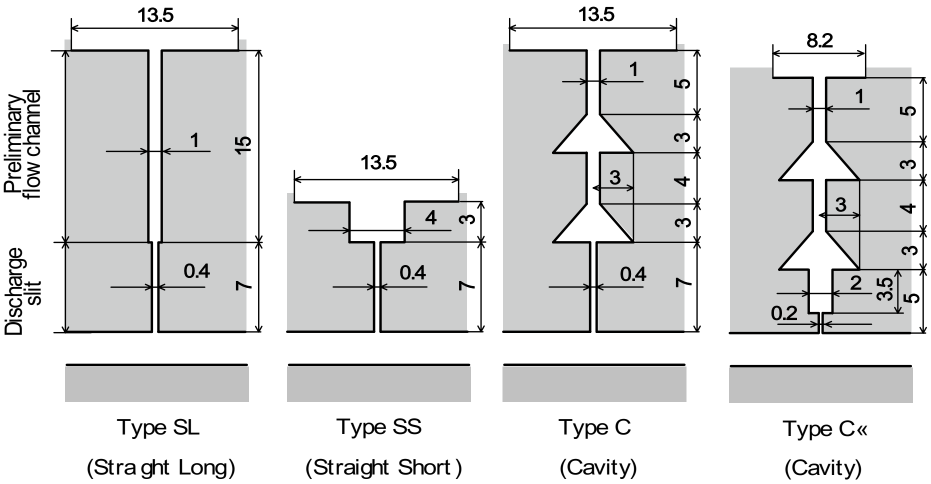

(b) Detail of nozzle shape

Fig. 1. Experimental apparatus

a slit of 0.4mm width and 7mm depth at the exit. The C' nozzle was manufactured as a trial to improve the performance of the C nozzle. The slit of the C' nozzle has a 0.2mm width to reduce the flow rate and has only 1.5mm depth to avoid the attenuation of turbulence generated in the cavity.

2.2 Measurement method for air velocity

In this study, we measured two types of air velocity: u and v, defined as the velocity of the horizontal airflow along the test plate and the downward air jet ejected from the discharge slit, respectively.

For the measurement of the horizontal velocity u, we used a Pitot tube anemometer as shown in Fig. 2. The static pressure was measured with a manometer (PG-100-102RP: Copal Electronics) attached to the pressure tap in the test plate. The total pressure of the airflow along the wall was also measured with the same type of manometer connected to a narrow stainless tube of 0.13mm I.D. and 0.31mm O.D. The tube was placed along the wall at a right angle to the discharge slit. The velocity was calculated from the static and total pressures, which were measured in the range of x=0-10mm, based on Bernoulli's principle. The Pitot tube anemometer used in this experiment had a slow response time, so time-averaged velocity ($\overline{u}$) readings were taken. The calculated value indicates the velocity at 0.16mm above the wall surface since the outer diameter of the stainless steel tube is 0.31mm.

When we measured the downward velocity v of the air jet, we used a hot-wire anemometer (Model

1010: Nihon Kanomax, Frequency response: 100 kHz). As shown in Fig.3, a hot-wire probe (0251R: Nihon Kanomax) was placed 1.5mm below the discharge slit, after taking away the test plate to provide enough space to insert the probe. In this experiment, we measured the average velocity and examined the velocity fluctuation generated by the nozzle just before the jet impinges on the wall. The probe was movable in the x direction using the traverser. The output from the hot-wire anemometer was recorded by a digital oscilloscope (9304AM: Lecroy) and processed to obtain time-averaged velocity ($\overline{v}$), turbulent intensity $\sqrt{\overline{v'^2}}$ and a frequency spectrum, where v' is the velocity fluctuation.

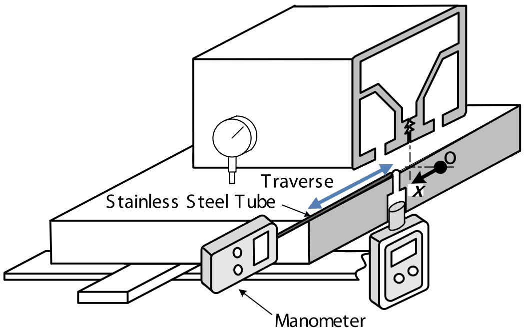

Fig. 2 Measurement method for horizontal air jet velocity along a test plate

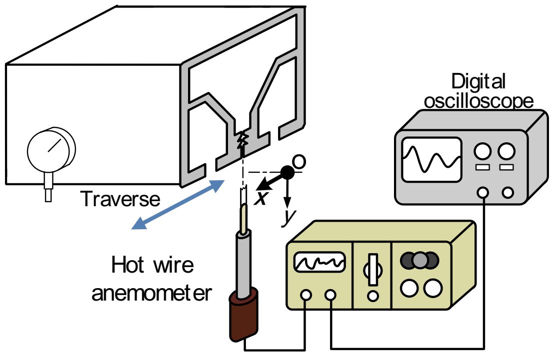

Fig. 3 Measurement method for downward air jet velocity

2.3 Measurement method for wall-pressure fluctuation

Figure 4 illustrates the method used to measure pressure fluctuation on the wall. A piezoelectric sensor (Model HSM113A28: PCB Piezotronics) with an excellent time response (Frequency response: 500 kHz) was attached to the pressure tap to measure the fluctuating pressure. The pressure tap was carefully designed not to spoil the time response. The dead space between the sensor and the pressure tap was minimized to the size of 1mm height and 5.6mm diameter. In addition, silicon oil of 1.0×10^6cSt kinematic viscosity (KF-96H: Shin-Etsu Chemical) was filled into the dead space and pressure tap. In order to remove bubbles in the oil, the oil was then held in a vacuum for a day at 50°.

To confirm the accuracy of the measurements obtained through the pressure tap, we measured the pressure fluctuation (p') that resulted from ultra sonic waves of 40 kHz (Generated by a device MA40B8S: Murata Manufacturing Company) measured with and without the pressure tap. The comparison is shown in Fig. 5. The p' measured through the pressure tap agrees well with that measured directly.

In the actual experiments, we recorded the measured wall-pressure fluctuation p' using a digital oscilloscope (9304AM: Lecroy) and processed it to obtain the intensity of the pressure fluctuation $\sqrt{\overline{p'^2}}$ and the frequency spectrum. The measurements of the velocity and pressure fluctuation described up to this point were taken without any micron-order particles being present.

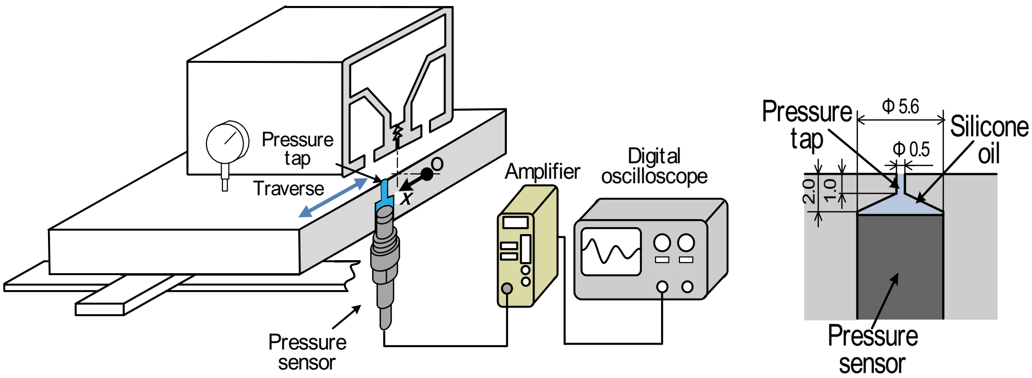

Fig.4 Measurement method for wall pressure fluctuation

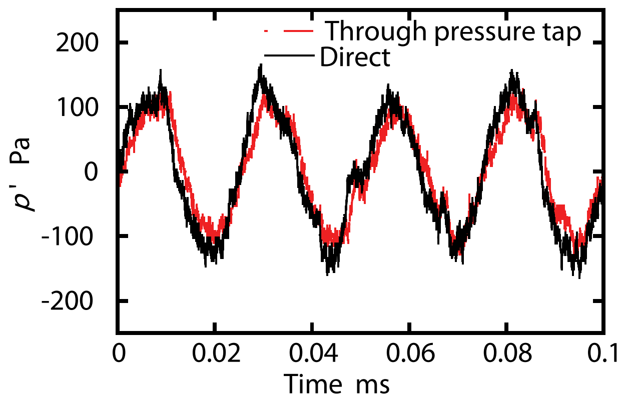

Fig. 5 Comparison of pressure fluctuations measured through pressure tap and measured directly

2.4 Measurement method for particle removal rate

We measured particle removal rate with a surface inspection device (GI-4600: Hitachi High-Technologies). Mono-disperse spheres of 1.6μm diameter made of silica-acryl complex (Soliostar: Nippon Shokubai) were used as a model of the fine particles. When we compared the removal ability between C and C' nozzles (section 4), 3μm particles were used as well as 1.6μm. We used a chromium-coated glass substrate as a test plate. Static electricity was eliminated on the test plate to limit the electrostatic forces that could bind the particles to the plate. The test plate, on which the model particles had been dispersed preliminarily, was conveyed in the *x* direction at the constant speed of 100 mm/s and was cleaned.

The removal rate was defined as $(n_a-n_i)/(n_b-n_i)$, where n_i is the number of initial adhesion particles on the glass plate before the spreading of the model particles, and n_b and n_a are the numbers of particles before and after cleaning, respectively. We repeated the measurement of removal rate 3 times for each experimental condition and averaged to determine the final measurement value.

3. RESULTS AND DISCUSSION

The experimental results for the three kinds of nozzles excluding C' are shown in this section, in order to investigate the factor that has the most significant effect on the particle removal. The comparison of measured results between C and C' will be stated in section 4.

3.1 Average velocity of jet and airflow along the wall

Figure 6(a) shows the distribution of the average downward velocity $\overline{v}$ of the air jet obtained for the three nozzles at P=11kPa. The horizontal and vertical axis represent the x-coordinate and $\overline{v}$ respectively.

Because we took off the test plate to place the hot-wire probe, we cannot accurately measure the downward velocity when it is affected by the plate. Despite this, measurements taken without the test

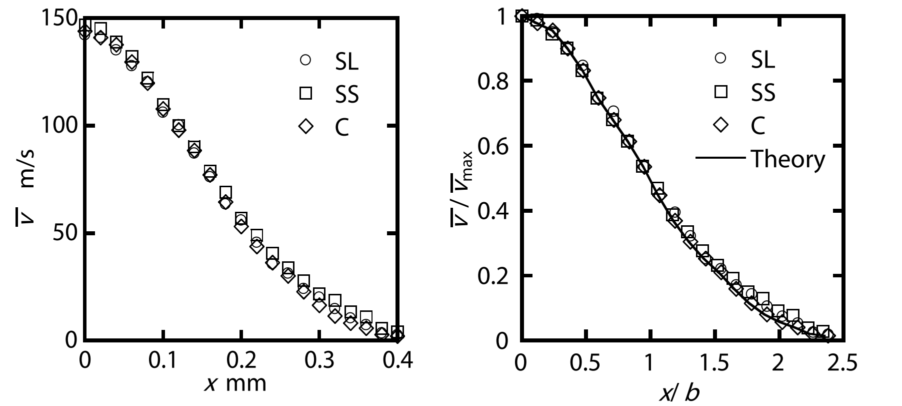

(a) Velocity distribution

(b) Comparison of measured velocity distribution with theoretical one

Fig. 6 Average downward velocity of air jet (P=11kPa)

plate are preferable as they allow us to measure the inherent characteristics of each nozzle without the plate affecting our readings.

Figure 6(a) shows that the average velocity $\bar{v}$ has a maximum value of 140m/s at x=0mm and that it decreases rapidly as x increases. $\bar{v}$ has a value of approximately 10% of the maximal velocity at x=0.3mm. As shown in Fig. 6(a), it was observed that the velocity distribution and maximum velocity were not related to the shape of nozzle. The same tendency was also obtained at P=8kPa and 14kPa.

The comparison of the measured velocities with the theoretical value of fully developed two-dimensional turbulent jet [9] is shown in Fig. 6(b). In order to normalize the horizontal and vertical axes, they were divided by b (The x-value when $\bar{v}$ is half its maximum velocity) and $\bar{v}$ max respectively. The measured velocities agree with the theoretical values although measuring point (y/b=3.75) is not so far from the discharge slit. It may be because jet velocity distribution at slit exit has already been developed.

Figure 7 shows the average horizontal velocity $\bar{u}$ of the airflow along the wall obtained at P=11kPa. The velocity $\bar{u}$ reaches a maximum at x=1mm regardless of nozzle shape, and then it decreases gradually with increasing x-values up to x=8mm. Finally, $\bar{u}$ reaches a constant value of about 20m/s at x≥8mm. Similar dependence of $\bar{u}$ on x was seen when P=8kPa and 14kPa. This distinctive dependence on x suggests the occurrence of contracted flow at x=0-8mm, which is probably due to the separation vortexes generated at both sides of the discharge slit. It should be noted that the maximum horizontal velocity $\bar{u}_{max}$ obtained at x=1mm has a value of 80% of the maximum downward velocity $\bar{v}_{max}$.

The variations in $\bar{u}_{max}$ and $\bar{v}_{max}$ by P are summarized in Fig. 8. $\bar{u}_{max}$ and $\bar{v}_{max}$ increase with increasing P monotonically. This distribution is not affected by nozzle shape.

Summarizing this section, it is concluded that the average velocities do not depend on nozzle shape although they do increase with increasing P.

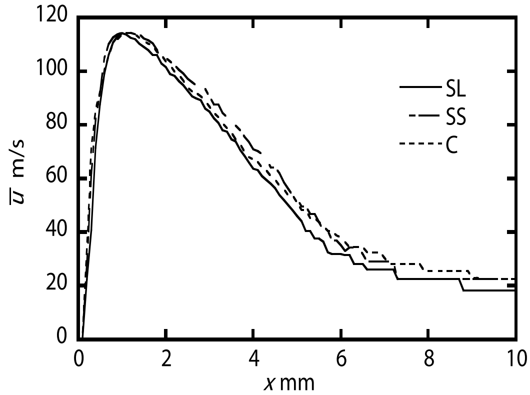

Fig. 7 Average horizontal velocity of airflow along the wall (P=11kPa)

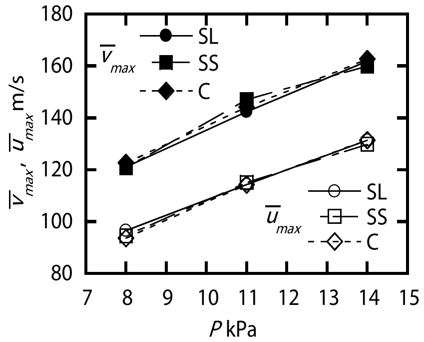

Fig. 8 Maximum average velocity at x=0mm

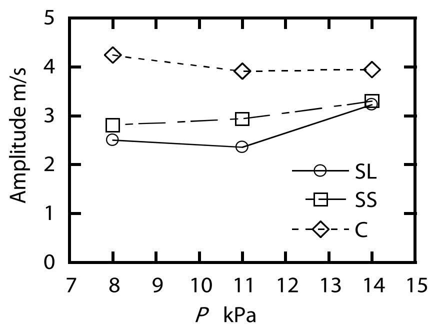

Fig. 9 Turbulent intensity of downward velocity of air jet measured at x=0mm

3.2 Turbulent intensity of downward velocity of air jet

Figure 9 shows the turbulent intensity of the downward velocity of the air jet measured at x=0mm. The turbulent intensity values (rms) for the three nozzles are plotted against P in Fig. 9, although it is necessary to keep in mind that the measurement of the downward velocity was performed without the test plate, as mentioned in sections 2.2 and 3.1.

The turbulent intensity is affected by the nozzle shape strongly as shown in Fig. 9, while the average velocities are independent of P. The C nozzle has the highest intensity among the three types of nozzles regardless of P, although the intensity of the C nozzle slightly decreases and the difference from the other two nozzles becomes smaller as P increases. This strong intensity may be due to the turbulence generated at the cavities in the C nozzle. The intensities observed in the SS and SL nozzles slightly increase with P and show a similar pattern to each other. The small difference between SS and SL nozzles suggests that nozzle length has little effect on the turbulent intensity. In addition, the turbulent intensities slightly increase as P increases for the SS and SL nozzles.

To investigate the dependence of turbulent intensity on the fluctuation frequency, we applied a Fourier transformation to the velocity v measured at x=0mm and P=11kPa. The frequency spectrums of the downward velocity for the three nozzles are shown in Fig. 10.

The spectrums for all nozzles have a broad frequency band up to 30 kHz. The C nozzle, in particular, shows larger amplitude especially at frequencies higher than 5 kHz. This indicates that the high frequency turbulence caused by the cavities contributes to the high turbulent intensity of the C nozzle as shown in Fig.9.

The results in this section lead to following conclusions: the turbulent intensity of the downward air jet has a strong dependence on nozzle shape, while it has little relation to P. In addition, the C nozzle has the largest intensity.

3.3 Wall pressure fluctuation

Figure 11 shows the intensity of wall-pressure fluctuation measured at x=0mm against P. The intensities for the SL and SS nozzles have almost the same values as each other and increase

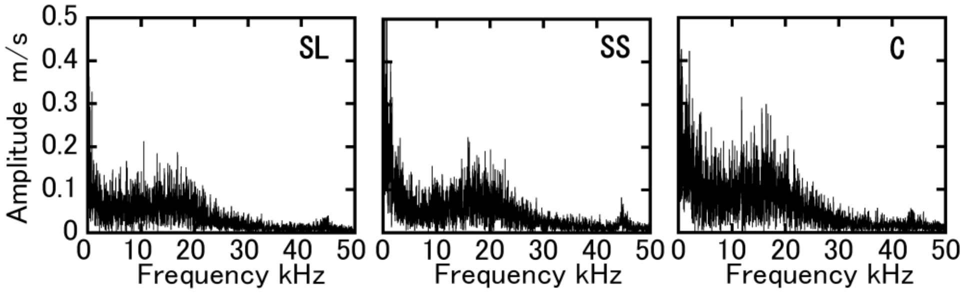

Fig. 10 Frequency spectrum of velocity fluctuation of downward air jet measured at x=0mm and P=11kPa

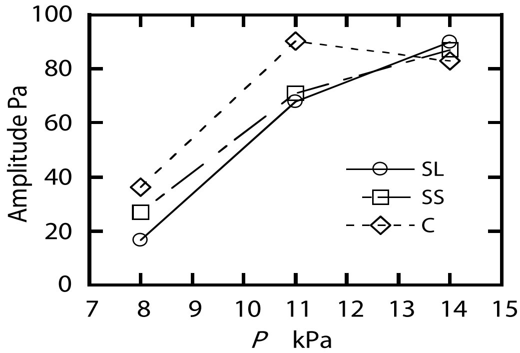

Fig. 11 Intensity of wall pressure fluctuation at x=0mm

monotonically with an increase in P, while that for the C nozzle has a peak at P=11kPa and then decreases slightly.

Therefore, although the intensities for the C nozzle are larger than those for the SL and SS nozzles at P=8 and 11kPa, all nozzles indicate almost the same fluctuation intensity at P=14kPa. This tendency is similar to that of the velocity fluctuation stated in 3.3, in which the difference of intensity becomes smaller at P=14kPa.

We calculated the frequency spectrums of the wall-pressure fluctuations measured for all three nozzles at x=0mm. The spectrums obtained at P=8, 11 and 14kPa are shown in Fig. 12(a), (b) and (c), respectively. The frequency band extends to about 40 kHz regardless of the nozzle shape and P.

In the case of the SL nozzle, the spectrum has a blunt peak between 30-40 kHz, which becomes more apparent at P=11 and 14kPa. In addition, spectral amplitude is intensified at all frequencies with increasing P. The spectral pattern of the SS nozzle is similar to that of the SL nozzle. This spectral similarity corresponds to the similarities of fluctuation intensity between the SL and SS nozzles, as shown in Fig.10. Because the similarity is slightly diminished at P=8kPa; fluctuation intensities and spectral amplitudes for the SL nozzle are a little smaller than those for the SS nozzle at P=8kPa.

On the other hand, the spectrum of the C nozzle has a prominent sharp peak at P=8 and 11kPa. The frequencies of the sharp peaks at P=8 and 11kPa are 10.4 kHz and 11.4 kHz, respectively. This monotone pressure fluctuation may be caused by the cavities.

The fluctuation frequency f generated at a cavity can be predicted by the theoretical formula, $f = (v_c / L) / (1 + v_c/a)$, where v_c is the flow velocity at the cavity, L is the length of the cavity and a is the acoustic velocity [8]. The air flow rate of the C nozzle was calculated by the integration of the distribution of downward velocity (See Fig. 6(a)). We estimated the value of v_c as 50.7 m/s. Using this value and the geometric form of the C nozzle we predicted the frequency at P=11kPa as 14.7kHz. Although this predicted frequency of 14.7 kHz is a little larger than the measured frequency 11.4 kHz, because of the rough estimation of v_c, both are approximately the same.

Considering the relationship between the pressure fluctuation intensity and frequency spectrum, the fluctuation intensity of the C nozzle becomes larger than that of the other nozzles when the sharp peak appears in the spectrum. This means that the sharp peak contributes to the fluctuation intensity.

Comparing Fig. 12(b) with Fig.10, we can find no sharp peak for the C nozzle in Fig. 10. This fact indicates that the pressure fluctuation does not result from the velocity fluctuation, but from the acoustic wave instead. The following experimental facts also support this interpretation. Firstly we obtained similar spectrums to Fig. 12 even when we covered the pressure tap with a thin plastic plate. In addition, the spectrum of the acoustic wave recorded with a microphone which was located far from the airflow, showed the same peak and distribution as Fig. 12.

The results in this section lead to the conclusion that the sharp peak found in the spectrum of pressure fluctuation for the C nozzle originates from the acoustic wave generated at the cavities. This sharp peak increases the intensity of the wall-pressure fluctuation. Despite this, the reason why the sharp peak disappears at P=14kPa is not clear, although the interaction between the wall and the jet is a possible cause. It is a subject to investigate further in the future.

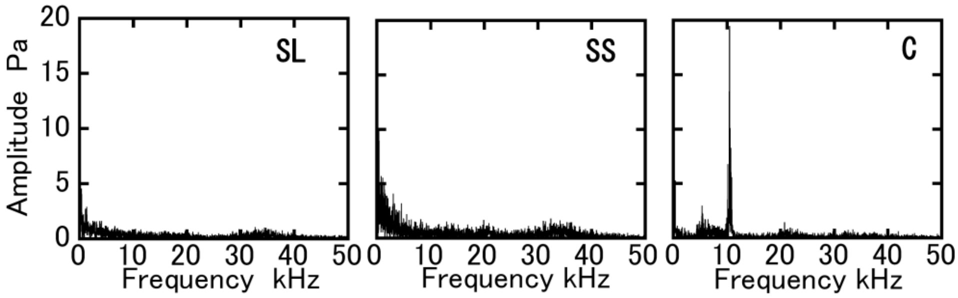

(a) P=8kPa

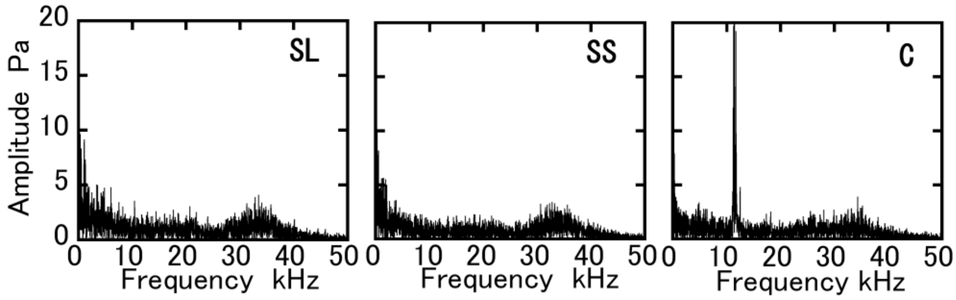

(b) P=11kPa

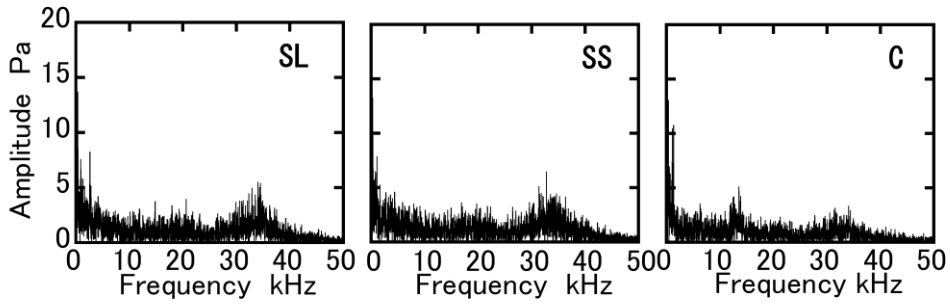

(c) P=14kPa

Fig. 12 Frequency spectrum of wall pressure fluctuation at x=0mm

3.4 Particle removal rate

Figure 13 shows the variation of particle removal rate γ with P. The measured results of γ increase monotonically with P. The C nozzle has the highest value at each P, although the difference becomes smaller as P increases. It is natural that the removal performance will be better as the pressure increases, since the jet impinging velocity increases with P as shown in Fig. 8. On the other hand, γ is dependent on nozzle shape even at the same jet velocity. For this reason, the effect of fluctuation given by the nozzle can be considered. Actually the experimental results of velocity and pressure fluctuations show similar behavior to γ in the sense that the fluctuations of the C nozzle are largest although the difference between the three kinds of nozzles becomes close to each other as P increases. The particle removable rate can be improved by the pressure or velocity fluctuation of high frequency as well as the impinging jet velocity. Concerning the pressure fluctuation, a prominent sharp peak was observed, as shown in the power spectrum of Fig.12. The effect of this acoustic pressure fluctuation on the particle removal is supported by a demonstration Peri and Cetinkaya gave [10]. They proved that a single micro-sphere can be excited into a swinging motion by means of an acoustic wave.

It can be concluded that the cavity installed in the C nozzle has an efficient influence on the particle removable rate through the generation of high frequency pressure or velocity fluctuations.

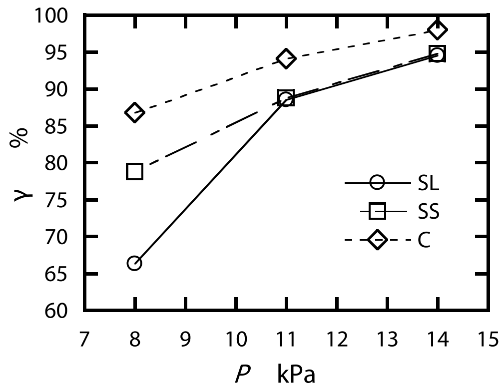

Fig. 13 Particle removal rate

4. EXAMINATION OF THE FLOW RATE REDUCTION

The jet velocity, velocity fluctuation and removal rate were measured for the low flow rate type of C' nozzle (slit width 0.2mm) at P=14kPa, and the results were compared with those for the other nozzles (slit width 0.4mm) shown in the preceding section. Although the contribution of pressure fluctuation to particle removal is also expected for C' nozzle, the pressure tap of 0.5mm diameter cannot detect the pressure fluctuation generated by the C' nozzle with the very small slit width of 0.2mm correctly. Therefore, only the velocity fluctuation is discussed in this section.Table 1 shows the maximum velocity, rms of velocity fluctuation at x=0 mm and the removal rate for 3μm and 1.6μm particles. As shown in the table, the jet velocity of the C' nozzle is about 20% smaller than that of other nozzles, while the velocity fluctuation is conversely more than twice the others. The particle removal rate of the C' nozzle is comparable with C and higher than the other two types of nozzles. These results again indicate that the turbulence included in the jet flow has a strong influence on the particle removable rate. Since the slit depth of C' is quite short (1.5mm) as compared with that of C (7mm), as stated in 2.1, the turbulence generated at the cavity may be preserved strongly in the C' nozzle and the removal rate is improved in spite of the low jet velocity.

In this experiment, we have examined the particle removal performance of the C' nozzle using the same cavities as the C nozzle while a reduced flow rate. The experimental results show that the C' nozzle had a similar performance even under the condition of less than half the air flow rate as the C nozzle.

Table 1 Removal rate γ for two kinds of slit width (P=14kPa)

Nozzle type	C'	C	SS	SL
Slit width (mm)	0.2	0.4	0.4	0.4
Jet velocity (m/s)	135	162	160	161
Velocity fluctuation (m/s)	8.9	3.9	3.3	3.2
Removal rate for 1.6 μm (%)	99.7	98.0	94.8	94.5
Removal rate for 3.0 μm (%)	99.2	99.0		

5. CONCLUSION

We measured the velocities of the downward air jet and the horizontal airflow along the wall, the wall-pressure fluctuation, and the particle removal rate using the four types of nozzle in order to discover which had the largest effect on particle removal. The following conclusions were derived from the results and discussion:

1. Average velocities of the downward air jet and the horizontal airflow increase with increasing P. However, they do not depend on nozzle shape.
2. The turbulent intensity of the downward air velocity has little relation to P, while it has a strong dependence on nozzle shape. That of the C nozzle is the largest of all nozzles.

3. The intensity of the wall-pressure fluctuation for the SL and SS nozzles increases as *P* increases. On the other hand, the intensity of the C nozzle increases up to P=11kPa, and then remains constant at $P \geq$11kPa. Additionally, the C nozzle has the largest intensity. This dependency on *P* is different from that of velocity turbulent intensity because wall-pressure fluctuation does not result from the velocity fluctuation but from the acoustic wave generated in the nozzle instead.
4. The particle removal rate increases with *P* and is largest for the C nozzle having the greatest pressure and velocity fluctuations. The high frequency turbulence generated by the cavity has a positive effect on the particle removal rate.
5. The C' nozzle with a narrow slit was manufactured to examine the performance of a nozzle having the same cavity size as the C nozzle under a low flow rate condition. The experimental results showed that the particle removal rate is comparable to that of the C nozzle. This result again indicates that the particle removal performance is strongly related to the magnitude of turbulence included in the jet flow.

REFERENCE

[1] K, Gotoh., S, Takebe., H, Masuda. and Y, Banba., The Effect of Humidity on the Removal of Fine Particles on a Solid Surface Using a High-Speed Air-jet (in Japanese), *Kagaku Kogaku Ronbunshu*, vol.20,No.2,1994, pp. 205-212

[2] K, Gotoh., S, Takebe. and H, Masuda., Effect of Surface Material on Particle Removal Using High Speed Air Jet (in Japanese), *Kagaku Kogaku Ronbunshu*, vol.20, No.5,1994, pp.685-692.

[3] K, Gotoh., M, Kida. and H, Masuda., Effect of Particle Diameter on Removal of Surface Particles Using High Speed Air Jet Effect of Surface Material on Particle Removal Using High Speed Air Jet, *Kagaku Kogaku Ronbunshu*, vol.20, No.5,1994, pp.693-700.

[4] K, Gotoh., M, Tagaya. and H, Masuda., Mechanism of Air Jet Removal of Particles (in Japanese), *Kagaku Kogaku Ronbunshu*, vol.21, No.4,1995, pp.723-730.

[5] Y, Otani., H, Emi., T, Morizane. and T, Mori., Removal of Fine Particles from Wafer Surface by Pulse Air Jets (in Japanese), *Kagaku Kogaku Ronbunshu*, vol.19, No.1,1993, pp.114-119.

[6] N, Namiki., Y, Otani. and H, Emi., Removal of Fine Particles from Various Surface by Consecutive Pulse Air Jets (Prediction of Particle Removal Efficiency with Resuspension Parameter) (in Japanese), *Kagaku Kogaku Ronbunshu*, vol.24, No.1,1998, pp.86-92.

[7] Schlosser, U., Bahners, T. and Schollmeyer, E., Some Remarks on the Removal of Adhered Particles by Oscillating Air Flows, *Journal of Adhesion Science and Technology*, vol.23,2009, pp.787-798.

[8] O, Mochiduki., Y, Maruta.,Ryuutaion Kougaku Nyumon (in Japanese), *Asakura Shoten* ,1996, 89-91.

[9] Schlichting, H., Boundary-Layer Theory 7th ed., *McGraw-Hill*,1979, pp. 745-747.

[10] Peri, M, D, Murthy. and Cetinkaya, C., Air-coupled Excitation of Rocking Motion of Individual Microspheres on Surfaces, *Applied Physics Letters*, Vol. 90,No.17,2007, 171906.1-171903.3.